IEEE Access
Multidisciplinary ⋮ Rapid Review ⋮ Open Access Journal

Received February 25, 2021, accepted March 14, 2021, date of publication March 17, 2021, date of current version March 26, 2021.

Digital Object Identifier 10.1109/ACCESS.2021.3066638

Wideband Transmissive Polarization Rotator With In-Band Notches Enabling Multiband Operation

AHMED ABDELMOTTALEB OMAR[1], (Member, IEEE), ABDELHADY MAHMOUD[2], JAEHONG CHOI[1], (Student Member, IEEE), AND WONBIN HONG[1], (Senior Member, IEEE)

[1]Department of Electrical Engineering, Pohang University of Science and Technology, Pohang 37673, South Korea
[2]Faculty of Engineering, Benha University, Benha 13512, Egypt

Corresponding authors: Abdelhady Mahmoud (abdoeng78@gmail.com) and Wonbin Hong (whong@postech.ac.kr)

This work was supported by the Next Generation Engineering Research Program of National Research Foundation of Korea (NRF) through the Ministry of Science, ICT, under Grant 2019H1D8A2106519.

ABSTRACT A low-profile and wideband transmissive polarization rotator is proposed in this article. The wideband performance is accomplished by utilizing a curved bowtie resonator. The proposed wideband design exhibits a simulated bandwidth of 129.07% for at least 90% cross-transmission coefficient. The operating bandwidth is from 22.8 GHz to 105.8 GHz and the structure thickness is 0.082 λ_{max}, where λ_{max} is the free-space wavelength at the lowest operating frequency. A comparison with previously reported wideband polarization rotator designs is performed to highlight the notability of the proposed design regarding the wideband performance and structure thickness. In addition, in-band notches are utilized within the wide operating band to accomplish a transmissive polarization rotator with multiple operating bands. Single and double notches are employed to achieve polarization rotator designs with dual- and tri-band of operation, respectively. Moreover, the proposed multiband technique enables bandwidth adjustment. The prototype is fabricated and experimentally studied and is found to be highly correlated to the numerical estimation.

INDEX TERMS Multiband, polarization conversion, transmissive polarization rotator, wideband.

I. INTRODUCTION

A transmissive polarization rotator is a structure capable of transmitting and converting the polarization of the incident electromagnetic wave by 90° within a certain frequency band. The transmission-type polarization rotators are instrumental for applications that require separation of wave polarization such as polarimetric imaging radar or radiometers, radars, transmitarray antenna, and filtennas [1]. Several techniques were utilized in previous literatures to implement transmissive polarization rotators, as detailed in [2]. In detail, there are examples such as multilayer inclined wire grids [3] and [4], cascaded meander lines [5], substrate integrated waveguide [6]–[9], and 45° twisted resonator sandwiched between two orthogonal wire grid layers [2], [10]–[15]. Utilizing the last technique, wideband transmissive polarization rotators were realized by employing zigzag-shaped resonator [12] while achieving 99% operating bandwidth. In [13], 92.6% operating bandwidth was accomplished by utilizing a single split-ring resonator. Elliptic and double split-ring resonators were employed [2] to achieve 115% and 119.5% bandwidths, respectively. However, the structure was relatively thick and unstable due to the exitance of air gaps between layers. In this article, a very wideband and stable transmissive polarization rotator is proposed. The proposed design employs a curved bowtie resonator in between two orthogonal wire grid layers. Moreover, this enables a much thinner topology in comparison to previous studies, which becomes advantageous for real-life applications.

A multiband transmissive polarization rotator was reported in [2] utilizing multiple strip resonators. Each resonator was responsible for each frequency band. In this article, a new technique that involves generating band notches within the operating spectrum is presented. By doing so, a multiband transmissive polarization rotator is accomplished and by tuning the position of the notches, the bandwidth of each

The associate editor coordinating the review of this manuscript and approving it for publication was Chinmoy Saha.

transmission band can be independently adjusted. The novelties of this article are summarized as follows.

1) A thin and wideband transmissive polarization rotator is proposed employing a well-designed curved bowtie resonator.
2) A new technique to accomplish multiband response is also reported for the first time. This technique employs the wideband design in point#1 along with vertically oriented strip resonators operate as band notches.
3) Easy design, easy tuning, and mechanical stability are considered as advantages of the newly proposed technique.

The evolution process of the proposed design is presented along with a performance comparison with designs reported in the literature. In addition, the multiband topology is proposed, fabricated, and measured. Finally, a conclusion is presented.

II. WIDEBAND TRANSMISSIVE POLARIZATION ROTATOR

A. WIDEBAND UNIT CELL

Fig. 1(a) illustrates the 3D view of the proposed wideband transmissive polarization rotator unit cell and array structure. The detailed dimensions including the lamination details are also shown in the figure. The unit cell consists of three copper layers, the first layer is copper wire grids oriented in the y-direction, which only transmits the x-polarized wave. The second layer is the 45° tilted curved bowtie resonator and this layer determines the overall performance of the rotator. The operating mechanism of the presented polarizer maybe simplified as shown in Fig. 1(b). The x-polarized wave that passed through the first layer is decomposed into two perpendicular components due to the existence of the 45° tilted curved bowtie resonator, as shown in Fig. 1(b). One component is parallel to the 45° tilted curved bowtie resonator, while the other component is perpendicular. The parallel component is reflected back to the first layer, at which it is decomposed into two components then reflects the y-polarized component to the middle layer and so on. The perpendicular component to the 45° tilted curved bowtie resonator is transmitted to the third layer and the y-polarized component can pass through it. Although the conversion efficiency of the middle layer is not that high, multiple reflections enable the total efficiency of the whole structure to be very high, as shown in Fig. 1(c). The simulated S-parameters are demonstrated in Fig. 1(c), which are obtained by using the full-wave simulator CST Microwave Studio and high-frequency structure simulator (HFSS). To mimic an infinite periodic structure, the periodic boundary conditions are applied along x- and y-directions of the unit cell. The proposed transmissive polarization rotator exhibits a bandwidth of 129.07% from 22.8 GHz to 105.8 GHz with at least 90% cross-transmission. The thickness of the structure equals 0.082 λ_{max}, where λ_{max} is the free space wavelength at the lowest operating frequency.

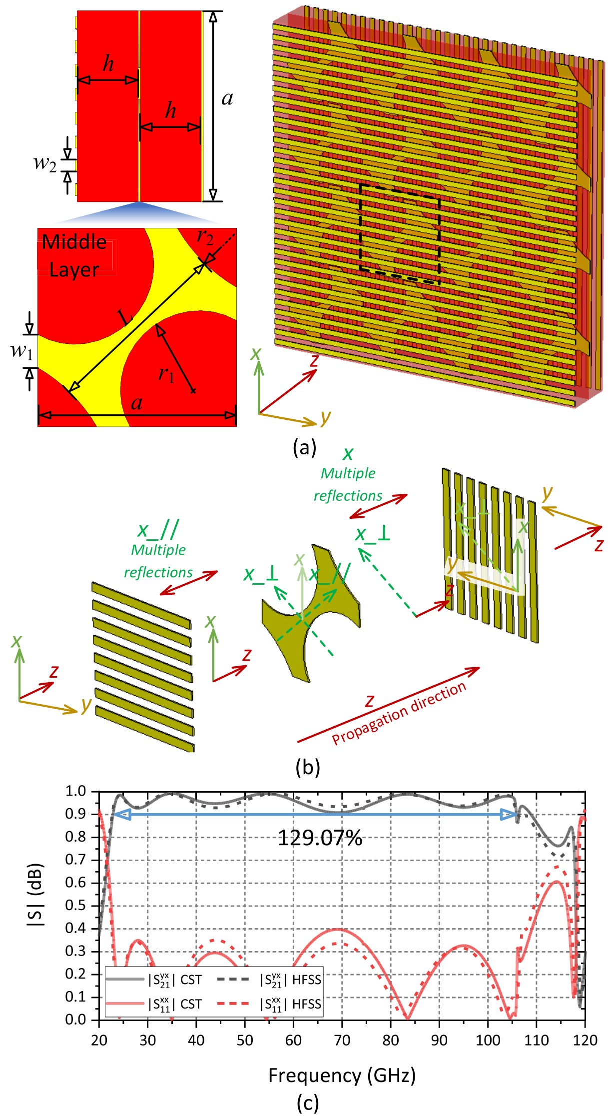

FIGURE 1. (a) Detailed unit cell dimensions and 3-D structure view of the proposed wideband transmissive polarization rotator. (b) Simplified explanation of the rotation mechanism. (c) Simulated co-reflection and cross-transmission coefficients under normal incidence ($a = 1.6$ mm, $\varepsilon_r = 3.5$, $h = 0.51$ mm, $L = 1.5$ mm, $w_1 = 0.267$ mm, $w_2 = 0.1$ mm, $r_1 = 0.6$ mm, $r_2 = 0.75$ mm).

B. EVOLUTION PROCESS

The evolution process of the middle resonator is illustrated in Fig. 2. It starts with a strip resonator reported in [11], which produces a single band at 60 GHz when its length is equal to $\lambda_g/2$, where λ_g is the guided wavelength. The operating band is enlarged, and its lower edge is reduced by employing an arrow bowtie resonator. The upper edge of the operating band is shifted forward by creating short resonators at the corners of the curved bowtie.

A comparison between the proposed design and designs reported in the previous literature is conducted and presented in Table 1. The proposed design exhibits the widest operating bandwidth with the thinnest structure. Mechanical stability is also satisfied in the proposed design since there are no

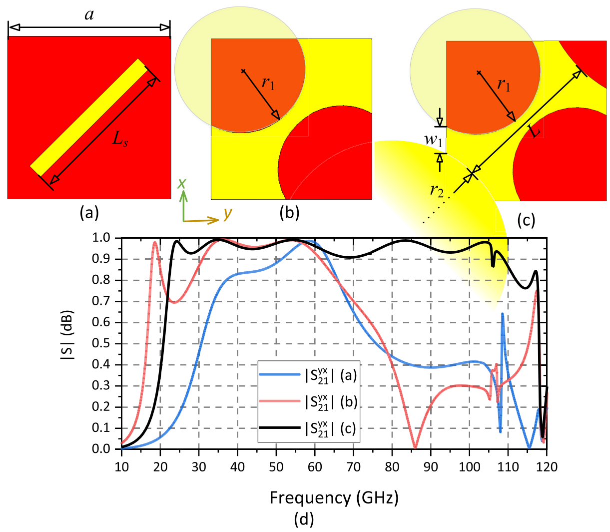

FIGURE 2. **(a) Strip resonator. (b) Arrow bowtie resonator. (c) Proposed resonator. (d) Simulated cross-transmission coefficient under normal incidence ($a = 1.6$ mm, $\varepsilon_r = 3.5$, $h = 0.51$ mm, $L_S = L = 1.5$ mm, $w_1 = 0.267$ mm, $w_2 = 0.1$ mm, $r_1 = 0.6$ mm, $r_2 = 0.75$ mm).**

TABLE 1. **Simulated comparison between the proposed wideband transmissive polarization rotator design and other designs reported in the previous literature (Ref.: Reference, BW: Bandwidth, $t_{structure}$: Structure thickness, UC_{size}: Unit cell size).**

Ref.	Freq. range (GHz)	BW (%)	$t_{structure}$ (λ_{max})*	UC_{size} (λ_{max})*	# dielectric layers	Structural stability
[12]	9.5-28.2	99	0.1	0.13	Two dielectric layers with no air spacers	Stable
[13]	4.4-12	92.6	0.12	0.16	Three dielectric layers with two air spacers	Unstable
[15]	170-390	78.6	0.08	0.23	Two dielectric layers with no air spacers	Stable
[2], Fig. 6	4.1-15.2	115	0.12	0.21	Three dielectric layers with two air spacers	Unstable
[2], Fig. 7	3.7-14.7	119.8	0.13	0.19	Three dielectric layers with two air spacers	Unstable
This work	22.8-105 .8	129	0.082	0.12	Two dielectric layers with no air spacers	Stable

* λ_{max} is defined as the free-space wavelength at the lowest operating frequency.

air layers, which makes the proposed design suitable for practical applications. In addition, the proposed unit cell size is relatively small compared with the reported designs in the literature.

III. MULTIBAND TRANSMISSIVE POLARIZATION ROTATOR

A. DUAL-BAND UNIT CELL

In this section, a multiband transmissive polarization rotator is proposed. By producing one and two notches within the operating bandwidth of the previously proposed wideband design, dual- and tri-band transmissive polarization rotators are accomplished, respectively. The main idea is to insert a bandstop resonator in front of the curved bowtie resonator. Fig. 3(a) shows the 3-D view of the dual-band unit cell. The front and back layers are wire grid layers orthogonally oriented to each other. The second layer is a single strip resonator oriented in the x-direction to produce a single notch within the wideband transmissive rotator bandwidth, which is produced by the curved bowtie resonator. The employed bowtie resonator is the same as the one utilized in Fig. 1. The simulated S-parameters are shown in Fig. 3(b). When the length of the strip resonator equals 1.3 mm, simulated bandwidths of at least 90% cross-transmission of the resultant dual-band transmissive rotator are 33.9% and 53.6% for the first and second bands, respectively. The vector surface current distribution at 52 GHz is shown inset of Fig 3(b). It is clear that the strip resonator is responsible to produce that notch. By changing the strip's length, the location of the notch can be tuned, hence, the bandwidths of the two bands are also tuned.

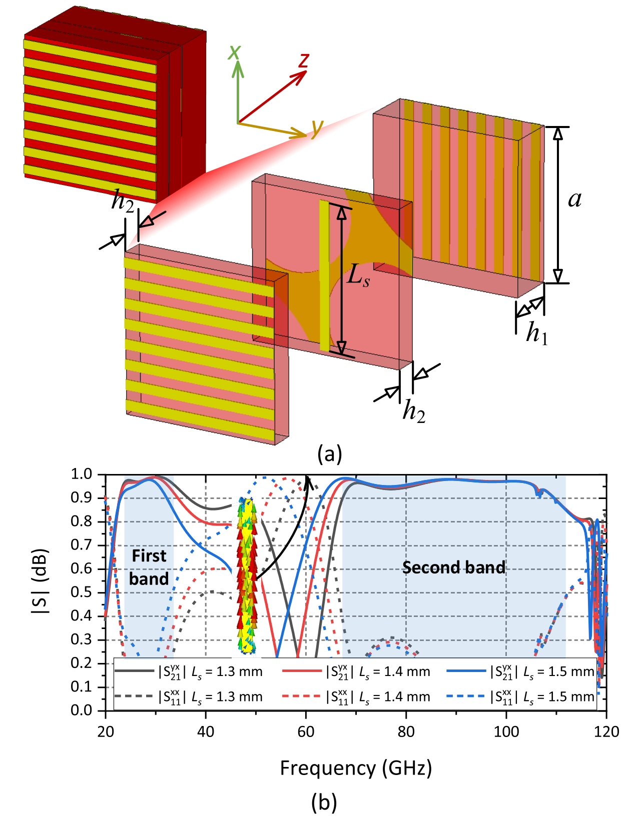

FIGURE 3. **(a) Proposed dual-band transmissive polarization rotator. (b) Simulated co-reflection and cross-transmission coefficients under normal incidence for different L_S value (inset, simulated vector surface current distribution at 60 GHz) ($a = 1.6$ mm, $\varepsilon_r = 3.5$, $h_1 = 0.51$ mm, $h_2 = 0.25$ mm, $L = 1.5$ mm, $w_1 = 0.267$ mm, $w_2 = 0.1$ mm, $r_1 = 0.6$ mm, $r_2 = 0.75$ mm).**

B. TRI-BAND UNIT CELL

The tri-band polarization rotator is accomplished by introducing another band notch with a different resonant frequency, as

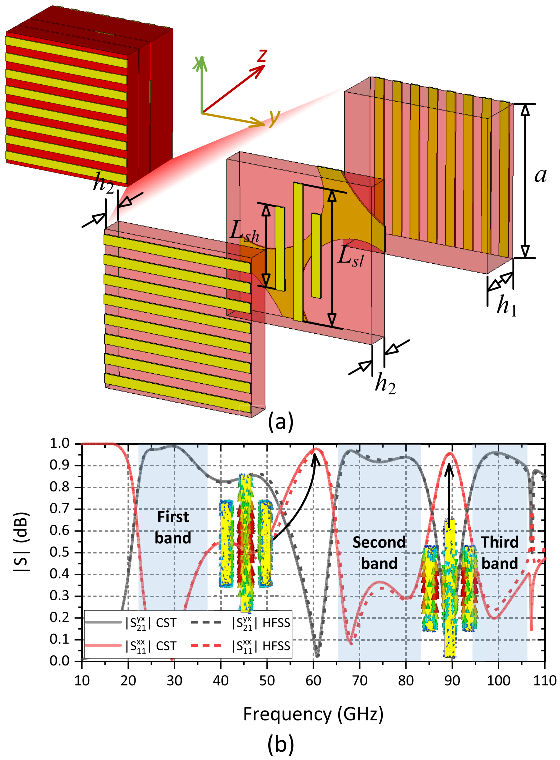

FIGURE 4. **(a) Unit cell details of the proposed tri-band transmissive polarization rotator. (b) Simulated co-reflection and cross-transmission coefficients under normal incidence (inset, simulated vector surface current distributions at 60 and 89 GHz) ($a = 1.6$ mm, $\varepsilon_r = 3.5$, $h_1 = 0.51$ mm, $h_2 = 0.25$ mm, $L_{Sl} = 1.3$ mm, $L_{Sh} = 0.85$ mm, L = 1.5 mm, $w_1 = 0.267$ mm, $w_2 = 0.1$ mm, $r_1 = 0.6$ mm, $r_2 = 0.75$ mm).**

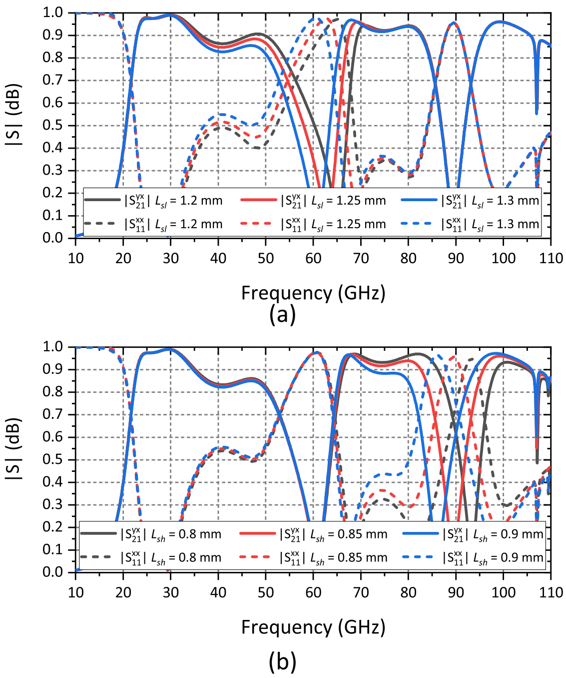

FIGURE 5. **Simulated co-reflection and cross-transmission coefficients under normal incidence. (a) Different L_{Sl} value and $L_{Sh} = 0.85$ mm. (b) Different L_{Sh} value and $L_{Sl} = 1.3$ mm.**

shown in Fig. 4. Three bands of 38%, 22.2%, and 9.8% bandwidths with 90% polarization conversion ratio are achieved.

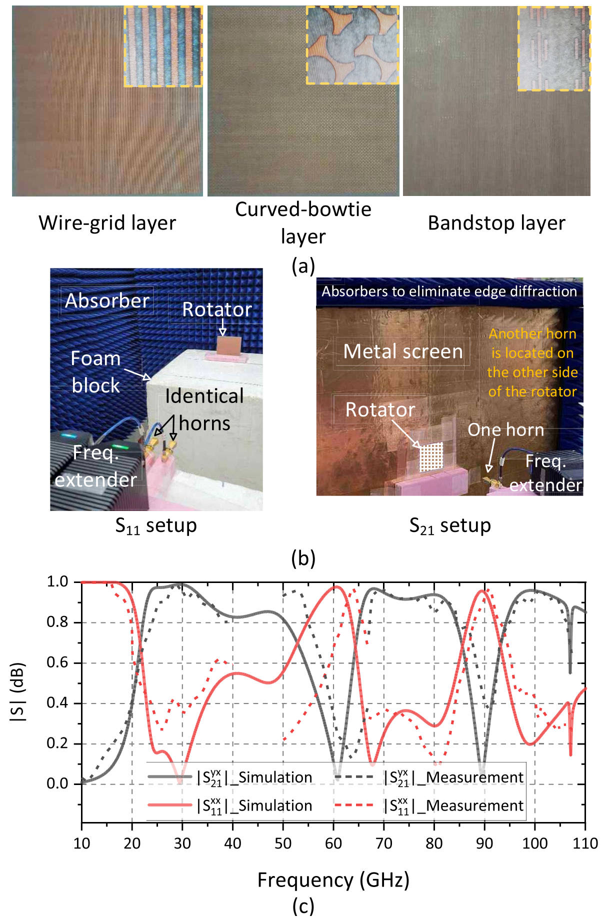

FIGURE 6. **(a) Photograph of the fabricated prototype. (b) Photographs of the measurement setup. (c) A comparison between the simulated and measured co-reflection and cross-transmission coefficients under normal incidence.**

These bandwidths may be adjusted by tuning the length of each strip to match the required operating bands. The simulated vector current distributions at the dual-band notch frequencies are shown inset of Fig. 4(b). It is clear that the lower frequency notch is produced by the long strip. In addition, the higher frequency notch is generated by the short strip. The bandwidth of the three bands can be simply controlled by changing the frequency location of both notches. The simulated co-reflection and cross-transmission coefficients for different L_{sl} and L_{sh} values are shown in Fig. 5.

C. FABRICATION AND MEASUREMENT

To validate the simulated results, the proposed tri-band transmissive polarization rotator design is fabricated and measured. Fig. 6(a) shows the 2-D view of the fabricated layers, wire-grid, curved-bowtie, and bandstop layer. The size of the fabricated structure is approximately 96 mm × 96 mm, which consists of 60 × 60 unit-cells. Taconic RF-35TC material [16] is used as the substrate material ($\varepsilon_r = 3.5$, $\tan\delta = 0.0011$ @ 10 GHz). It is worth mentioning that during simulation, the frequency dispersive characteristics of the dielectric material were incorporated to get accurate results. The measurement setups for both co-reflection and cross-transmission coefficients are shown in Fig. 6(b). In co-reflection measurement, both horns are utilized with the same polarization. While in cross-transmission situation, the polarization of both horns is perpendicular to each other's. A comparison between the measured and the simulated co-reflection and cross-transmission coefficients under normal incidence is shown in Fig. 6(c). Three sets of standard-gain horn antennas are used in the measurement. PowerLOG 40400 horn antenna is employed to cover the frequency range from 10 GHz to 40 GHz, the AT6024H horn antenna is utilized to cover the frequency range from 50 GHz to 67 GHz. To cover the rest frequency band, 67 GHz to 110 GHz, the LB-10-20-A horn antenna along with a frequency extender are employed. Due to the fabrication tolerance and measurement errors, marginal discrepancies between the measured data and simulated results exist.

IV. CONCLUSION

A stable and wideband transmissive polarization rotator has been proposed. A bandwidth of 129.07% from 22.8 GHz to 105.8 GHz has been accomplished. The development of the proposed unit cell originates from the strip resonator has been conducted. A comparison has been conducted with the reported polarization rotator designs in the literature. It is concluded that the proposed rotator design exhibits two advantages in terms of wideband characteristics and structural stability. A new technique to achieve a multiband polarization rotator has been introduced. By inserting band notches inside the wide operating band of the polarization rotator, multiple bands have been accomplished. The proposed tri-band polarization rotator design has been fabricated and successfully measured to validate the simulated estimations.

ACKNOWLEDGMENT

The authors would like to thank ANSYS Korea for their support. The authors would like to thank the anonymous reviewers for their comments and suggestions that led to improve the quality of this article.

REFERENCES

[1] M. Saikia, S. Ghosh, and K. V. Srivastava, "Design and analysis of ultrathin polarization rotating frequency selective surface using V-shaped slots," *IEEE Antennas Wireless Propag. Lett.*, vol. 16, pp. 2022–2025, 2017.

[2] A. A. Omar, Z. Shen, and S. Y. Ho, "Multiband and wideband 90° polarization rotators," *IEEE Antennas Wireless Propag. Lett.*, vol. 17, no. 10, pp. 1822–1826, Oct. 2018.

[3] N. Hill and S. Cornbleet, "Microwave transmission through a series of inclined gratings," *Proc. Inst. Elect. Eng.*, vol. 120, no. 4, pp. 407–412, Apr. 1973.

[4] N. Amitay and A. A. M. Saleh, "Broad-band wide-angle quasi-optical polarization rotators," *IEEE Trans. Antennas Propag.*, vol. AP-31, no. 1, pp. 73–76, Jan. 1983.

[5] T.-K. Wu, "Meander-line polarizer for arbitrary rotation of linear polarization," *IEEE Microw. Guided Wave Lett.*, vol. 4, no. 6, pp. 199–201, Jun. 1994.

[6] S. A. Winkler, W. Hong, M. Bozzi, and K. Wu, "Polarization rotating frequency selective surface based on substrate integrated waveguide technology," *IEEE Trans. Antennas Propag.*, vol. 58, no. 4, pp. 1202–1213, Apr. 2010.

[7] X.-C. Zhu, W. Hong, K. Wu, H.-J. Tang, Z.-C. Hao, J.-X. Chen, H.-X. Zhou, and H. Zhou, "Design of a bandwidth-enhanced polarization rotating frequency selective surface," *IEEE Trans. Antennas Propag.*, vol. 62, no. 2, pp. 940–944, Feb. 2014.

[8] J. Wang, Z. Shen, and W. Wu, "Cavity-based high-efficiency and wideband 90° polarization rotator," *Appl. Phys. Lett.*, vol. 109, no. 15, Oct. 2016, Art. no. 153504.

[9] M. S. M. Mollaei, "Narrowband configurable polarization rotator using frequency selective surface based on circular substrate-integrated waveguide cavity," *IEEE Antennas Wireless Propag. Lett.*, vol. 16, pp. 1923–1926, 2017.

[10] J. Wang, Z. Shen, X. Gao, and W. Wu, "Cavity-based linear polarizer immune to the polarization direction of an incident plane wave," *Opt. Lett.*, vol. 41, no. 2, pp. 424–427, Jan. 2016.

[11] N. K. Grady, J. E. Heyes, D. R. Chowdhury, Y. Zeng, M. T. Reiten, A. K. Azad, A. J. Taylor, D. A. R. Dalvit, and H.-T. Chen, "Terahertz metamaterials for linear polarization conversion and anomalous refraction," *Science*, vol. 340, no. 6138, pp. 1304–1307, Jun. 2013.

[12] Y. Li, J. Zhang, S. Qu, J. Wang, L. Zheng, A. Zhang, and Z. Xu, "Ultra-broadband linearly polarisation manipulation metamaterial," *Electron. Lett.*, vol. 50, no. 23, pp. 1658–1660, Nov. 2014.

[13] M. Saikia, S. Ghosh, S. Bhattacharyya, and K. V. Srivastava, "Broadband polarization rotator using multilayered metasurfaces," in *Proc. IEEE Appl. Electromagn. Conf. (AEMC)*, Dec. 2015, pp. 1–2.

[14] Z. Wei, Y. Cao, Y. Fan, X. Yu, and H. Li, "Broadband polarization transformation via enhanced asymmetric transmission through arrays of twisted complementary split-ring resonators," *Appl. Phys. Lett.*, vol. 99, no. 22, Nov. 2011, Art. no. 221907.

[15] X. Gao, L. Singh, W. Yang, J. Zheng, H. Li, and W. Zhang, "Bandwidth broadening of a linear polarization converter by near-field metasurface coupling," *Sci. Rep.*, vol. 7, no. 1, pp. 1–8, Jul. 2017.

[16] *Taconic RF-35TC Material*. Accessed: Oct. 10, 2020. [Online]. Available: http://www.taconic.co.kr/download/RF-35TC.pdf

AHMED ABDELMOTTALEB OMAR (Member, IEEE) was born in Giza, Egypt, in 1982. He received the B.Sc. and M.Sc. degrees in electrical engineering from Benha University, Benha, Egypt, in 2005 and 2010, respectively, and the Ph.D. degree in electrical engineering from Nanyang Technological University, Singapore, in 2019.

From 2007 to 2014, he was a Teaching Assistant with the Faculty of Engineering, Benha University. From 2012 to 2014, he was a Research Assistant with the Faculty of Engineering, Ain Shams University, Cairo, Egypt. He was a part-time Research Assistant with the School of Electrical and Electronic Engineering, Nanyang Technological University, from August 2018 to February 2019. In April 2019, he joined the Pohang University of Science and Technology (POSTECH), Pohang, South Korea, as a Postdoctoral Research Fellow. His current research interests include analysis and design of frequency-selective surfaces/structures, absorptive frequency-selective transmission/reflection structures, microwave absorbers; polarization rotators, and compact, wideband, and dual-polarized mm-wave 5G antennas.

Dr. Omar was a recipient of the Singapore International Graduate Award (SINGA) from the Government of Singapore to pursue his Ph.D. degree in 2014, the Best Student Paper Award 2018 (Honorable Mention) by the IEEE Singapore MTT/AP Joint Chapter-2018 Best Student Paper Contest, and shortlisted for the NTU-EEE Best Ph.D. Thesis Award 2019. In 2020, he won the 2020 POSTECH Initiative for Fostering Unicorn of Research and Innovation (PIURI) Fellowship. He serves as a regular reviewer for top-tier journals including the IEEE TRANSACTION ON ANTENNAS AND PROPAGATION, IEEE TRANSACTIONS ON MICROWAVE THEORY AND TECHNIQUES, IEEE TRANSACTIONS ON ELECTROMAGNETIC COMPATIBILITY, IEEE ANTENNAS AND WIRELESS PROPAGATION Letters, IEEE OPEN JOURNAL OF ANTENNAS AND PROPAGATION, and IEEE ACCESS.

ABDELHADY MAHMOUD received the B.Sc. (Hons.) and M.Sc. degrees in electrical engineering from Benha University, Benha, Egypt, in 2000 and 2005, respectively, and the Ph.D. degree in electrical engineering from Menoufia University, Egypt, in 2013.

From 2010 to 2012, he was a Ph.D. Researcher with the State Key Laboratory of Millimeter-Wave, Nanjing, China. From 2013 to 2015, he was a Postdoctoral Fellow with Concordia University, Montreal, QC, Canada. He is currently an Associate Professor with the Faculty of Engineering, Department of Electrical Engineering, Benha University. His current research interests include the design of RFID passive tags, artificial lens, circularly polarized, and linearly polarized reflectarrays and transmitarrays, MIMO, 3-D printed structure, broadband circularly polarized dielectric resonator antennas, and polarizer twisting structures at microwave and millimeter-wave frequencies.

JAEHONG CHOI (Student Member, IEEE) received the B.S. degree in electrical engineering from the Pohang University of Science and Technology (POSTECH), Pohang, South Korea, in 2018, where he is currently pursuing the unified M.S. degree. His current research interests include reconfigurable intelligent surfaces (RISs) and millimeter-wave/subterahertz ultrawideband array antenna for future 5G/B5G wireless systems.

WONBIN HONG (Senior Member, IEEE) received the B.S. degree in electrical engineering from Purdue University, West Lafayette, IN, USA, in 2004, and the master's and Ph.D. degrees in electrical engineering from the University of Michigan, Ann Arbor, MI, USA, in 2005 and 2009, respectively.

From 2009 to 2016, he was with Samsung Electronics as a Principal and a Senior Engineer. He is currently with the Department of Electrical Engineering, Pohang University of Science and Technology (POSTECH), Pohang, Republic of Korea, as an Associate Professor. He also holds the Mueunjae Chaired Professorship.

Dr. Hong received the ''Scientist of the Month'' by the Ministry of Science and ICT, and the National Research Foundation of Korea, in 2020. He also received an official commendation from the Minister of Science and ICT on the 55th Annual Invention Day hosted by the Korean Intellectual Property Office, in 2020. He was recognized for his contribution of inventing and commercializing the source technology on 5G millimeter-wave. His students have received numerous recognitions including the first Place Best Student Paper Award in IEEE AP-S Symposium on Antennas and Propagation, the IEEE European Conference on Antennas and Propagation (EuCAP), the Outstanding Master's Student, Electrical Engineering Department of POSTECH, the Silver Medal in the Samsung Electro-Mechanics Best Paper Award, the First Prize Best Student Paper Award in IEEE International Symposium on Antennas and Propagation (ISAP), and ISMOT. He is one of the first researchers to pioneer the concept and design of millimeter-wave antennas and RF front-ends in the field of consumer electronics for 5G communication. In addition, he is also an Inventor and served as the Project Lead for the world's first OLED/LCD display-embedded invisible antenna for three separate wireless connectivity applications. Owing to his accomplishments, he was promoted to the rank of Principal Engineer within the shortest period in the history of the business division at Samsung along with more than a dozen awards and recognitions during his career. He has served as an Invited Lecturer and a Speaker in over 80 international research symposiums, government and industry sessions held around the world. He is currently serving as the Associate Editor for the IEEE Transaction on Antennas and Propagation and *IEEE Antennas and Propagation Magazine*. He has also served as the Lead Guest Editor for the IEEE Antennas and Wireless Propagation Letters, Special Cluster on ''Antenna-in-Package, Antenna-on-Chip, Antenna-IC Interface: Joint Design and Co-Integration", from 2018 to 2019. From 2016 to 2017, he served as a Guest Editor for the IEEE Transaction on Antennas and Propagation Special Edition on ''Antennas and Propagation Aspects of 5G Communications.''